Computational Simulation of a Chiral Nonreciprocal Binary Mixture

Sergio Eraso
Department of Physics, Massachusetts Institute of Technology, Cambridge, MA 02139, USA
(Dated: May 17, 2024)

Nonreciprocity and chirality are increasingly popular topics within the field of nonequlibrium statistical physics. However, few studies have been dedicated to studying systems that posses both of these properties. Inspired by experimental work done at MIT with chiral starfish embryos, we carry out a computational model to explore the qualitative behavior of a chiral nonreciprocal binary mixture. While there is some qualitative agreement with experiment, it is limited. We observe phase separation in the low noise regime and quantify the dynamical coarsening of clusters for specific simulation parameters.

I. INTRODUCTION

In nature, being out of equilibrium is the norm rather than the exception. A booming field of nonequilibrium statistical mechanics research is active matter, the study of systems whose constituents break time-reversal symmetry via energy consumption [1]. These types of matter range across various length scales, from microscopic living cells and self-propelling colloids, to schools of fish and flocks of birds [1–3]. One type of active matter that breaks yet another symmetry: parity, are chiral self-rotating particles. Collections of such particles generically give rise to novel responses such as odd viscosity and elasticity [4, 5]. Macroscopic chirality is also a sign of nonequilibrium. For instance, consider a 2D conserved scalar field $\phi(x, y)$ obeying dissipative dynamics,

$$\frac{\partial \phi}{\partial t} = -\boldsymbol{\nabla} \cdot (\boldsymbol{J} + \boldsymbol{\eta}). \tag{1}$$

In general, the current $\boldsymbol{J}$ can be decomposed into the sum of curl and divergence-free pieces,

$$\boldsymbol{J} = -\boldsymbol{\nabla}\mu + \boldsymbol{\nabla} \times \boldsymbol{A} \tag{2}$$

where μ is often taken to be the derivative of some effective free energy and, without loss of generality, we let $\boldsymbol{A} = \hat{\boldsymbol{z}} A(x, y)$. This is so that the curl is restricted to the xy plane where ϕ is defined. Evidently, a system satisfying parity requires that $\boldsymbol{\nabla} \times \boldsymbol{A} = 0$, and it follows that there are no circulating currents in the expected state of the system, $\langle \boldsymbol{\nabla} \times \boldsymbol{J} \rangle = -\langle \boldsymbol{\nabla} \times \boldsymbol{\nabla}\mu \rangle = 0$. However, in the case of a chiral field, this term need not vanish, and the dynamical equations generically permit steady state solutions with circulating currents.

Active matter systems are also known to naturally give rise to effective nonreciprocal interactions – violations of Newton's action-reaction principle [5, 6]. While several studies has been done on chiral matter [7, 8] as well as non-reciprocal matter [6, 9, 10], comparatively less time has been devoted to systems that incorporate both properties.

One particular system of interest studied here at MIT are collections of spinning starfish embryos where theoretically predicted odd viscosity has been reproduced [11]. Binary mixtures (BM) of young, approximately isotropic, and old, elongated asymmetric, embryos have been experimentally observed to exhibit effective nonreciprocal interactions. Hydrodynamic interactions between spinning embryos lead to effective attraction and transverse forces [11]. These interactions lead to initially positionally disordered collections of BM embryos to eventually phase separate into a living chiral crystal (cluster) and gas of embryos, Fig. 1. Few experiments have been conducted for this complex system, so, to get an idea of the general behavior a chiral and nonreciprocal BM, we study a minimal computational simulation.

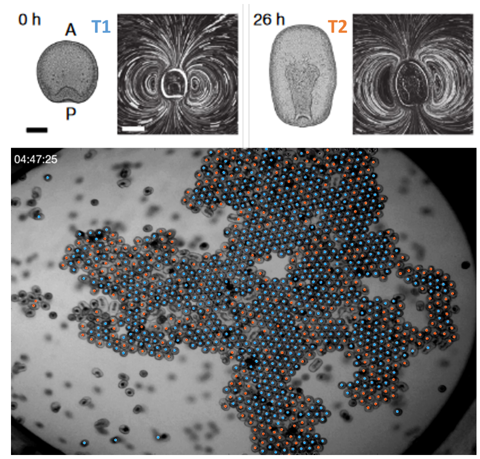

FIG. 1. (Upper) Two embryos at different developmental stages and their respective flow fields. Note the asymmetric shape of T2. (Lower) Snapshot of a living chiral crystal composed of two types of starfish embryos. Figure adapted from [11]

II. NUMERICAL SIMULATION

Motivated by the theoretical model in the supplement of [11], we simulate a dry mixture of two types of self-spinning particles in two-dimensional space with dimensions $L \times L$. As boundaries can have non-trivial effects on the behavior of non-equilibrium systems, we avoid these by working with periodic boundary conditions. For simplicity, both longitudinal and transverse forces follow

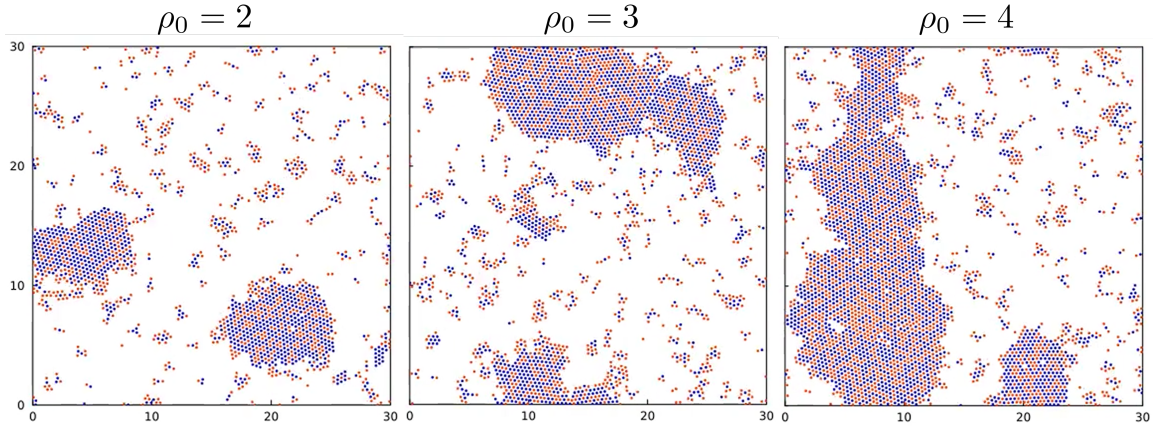

FIG. 2. Snapshots of the computer simulation for various densities. Colors correspond to different species.

Lennard-Jones shapes, whose parameters only change depending on the species of particles involved in the interaction. We work in the overdamped limit.

Each particle evolves as

$$\dot{\boldsymbol{r}}_i^\alpha = -\sum_{j\in 1} (\boldsymbol{\nabla} + \hat{\boldsymbol{z}} \times \boldsymbol{\nabla})\phi_{\alpha 1}(r_{ij}^1) \tag{3}$$

$$+\sum_{k\in 2} (\boldsymbol{\nabla} + \hat{\boldsymbol{z}} \times \boldsymbol{\nabla})\phi_{\alpha 2}(r_{ik}^2) + \eta \tag{4}$$

$$\phi_{\alpha\beta}(r) = \begin{cases} \frac{\epsilon_{\alpha\beta}}{4}\left[\left(\frac{\sigma_{\alpha\beta}}{r}\right)^{12} - \left(\frac{\sigma_{\alpha\beta}}{r}\right)^{6}\right] & r < 1 \\ 0 & r > 1 \end{cases} \tag{5}$$

where $\hat{\boldsymbol{z}}$ is the parity-breaking preferred axis of rotation and Greek indices take on values 1 or 2 corresponding to the types of Fig. 1. The quantity η is random Gaussian noise with zero mean and $\langle \eta_i(t)\eta_j(t')\rangle = 2D\delta_{ij}\delta(t-t')$. We further simplify the system by fixing the interaction strength $\epsilon_{\alpha\beta} = \epsilon$ and only introduce nonreciprocity via differing effective radii between cross-species interaction $\sigma_{12} \neq \sigma_{21}$. All simulations are initialized with particles arranged in a regular square lattice with random type assigned. For the rest of this paper, we fix $\sigma_{12} = \sigma_{11} = \sigma_{22} = 0.3$ and $\sigma_{21} = 0.33$. The ratio of nonreciprocal to reciprocal forces is

$$\frac{|\boldsymbol{\nabla}\phi_{21}|}{|\boldsymbol{\nabla}\phi_{12}|} \sim \left[1 + 2\left(\frac{\sigma_{12}}{r}\right)^6\right]\Delta \tag{6}$$

where $\Delta \equiv \sigma_{21} - \sigma_{12}$. This ratio is dependent on distance, so the system is nonconservative and it it is not possible to simply rescale the nonreciprocity away [10]. For the rest of the paper, we focus on the effect of varying the mean-field density $\rho_0 = (N_1 + N_2)/L^2$ with balanced number of species $N_1 = N_2$ in the low noise limit $\epsilon/D \gg 1$. Sample final states of these simulations are given in Fig. 2.

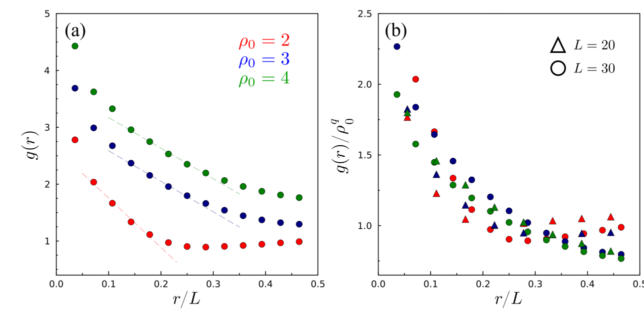

FIG. 3. (a) Time-averaged pair correlation functions at various mean-field densities for $L = 30$. (b) Pair correlation function after rescaling by the mean density for two simulation sizes.

III. DISCUSSION

To quantify the phase separation observed in Fig. 2, we calculate the pair correlation function $g(r) = \frac{1}{L^2}\sum_i \langle \delta(r_i - r)\rangle$. In the phase-separated state, we expect to see correlation behavior different than that for an order parameter like magnetization as the quantity we are dealing with, particle density, is conserved. Namely, phase separation is indicated by a linear trend, as depicted in Fig. 3 [12]. As we expect cluster size to increase with density, it is natural to rescale the data by ρ_0, for which we observe a collapse of the data upon further raising the density to a numerically estimated power $q \approx 1.2$. As there is no reason a priori for ρ_0 to be the only relevant scaling quantity – for instance, the ratio of species-specific density in each phase $\frac{\rho_1}{\rho_2}$ may also be a relevant order parameter – this maneuver will need a proper justification in future studies.

Next, we quantify the growth rate of clusters in the simulations. This was done using the DBSCAN algorithm which can identify an unspecified number of clusters via local density measurements [13]. We define the length-scale of a cluster $\ell(t)$ as the square root of its area. While this measurement poorly describes largely eccen-

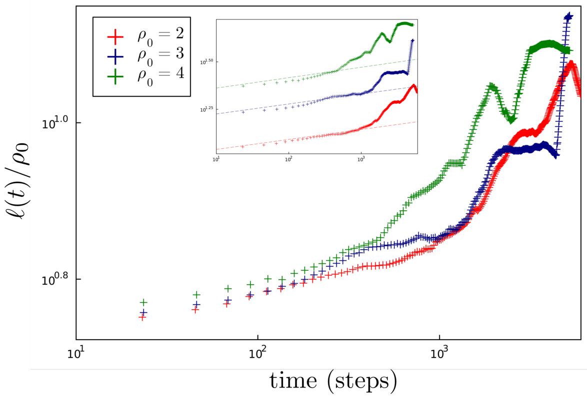

FIG. 4. Length scale of clusters rescaled by the mean-density $L = 30$. All data series follow the same power-law behavior at early times in the simulation. (inset) Unscaled series. Parameters: $D = 10^{-3}, \epsilon = 4$.

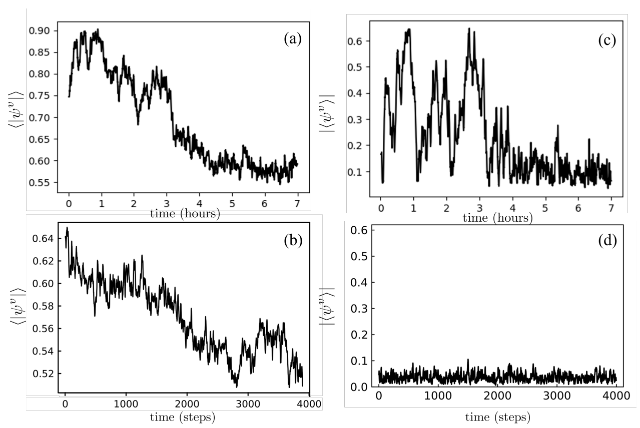

FIG. 5. (a)(c) Evolution from transient phase to phase separation is evident in the polarization for the experimental system, but not faithfully reproduced in the simulations (b)(d). (a)(c) Are from the experiment in Fig. 1 while (b)(c) are data from a $\rho_0 = 2$ simulation.

tric clusters, it provides a good estimate for short timescales when clusters are small and roughly circular. Clusters appear to coarsen according to a power law $\ell(t) \sim t^p$ for sufficiently short time scales where $p = 0.05 \pm 0.005$ (see Fig. 4). This is a clear manifestation of the active nature of the system and corresponds to much slower coarsening compared to purely passive diffusion which has $p = 1/3$ [14]. At long times, the merging and splitting of large clusters cause substantial variations in ℓ.

Lastly, we quantify the local ordering of the particles and compare to experimental measurements. To achieve this, we calculate each particle's polarization ψ^v, defined as

$$\psi^v = \frac{1}{n}\sum_i e^{i\theta_i^v}$$

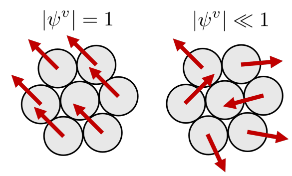

where the sum runs over nearest neighbors and θ_i^v is the phase of particle i's velocity. We observe qualitative agreement with experiment in $\langle|\psi^v|\rangle$ when going from the transient phase to the phase separated state Fig. 5. However, there is large disagreement in the absolute value of the mean polarization in both the transient and phase-separated states. In particular, the experiment seems to exhibit much stronger velocity alignment as well as clear spikes in polarization during the transient phase. This latter point is largely hindered in simulation where we have an interaction cutoff distance on the order of three particle radii.

IV. CONCLUSION

We have surveyed some features of a simple computational model inspired by experiments of nonreciprocal chiral starfish embryos. Even with untuned parameters, we were able to observe several qualitative agreements with experiment, such as phase separation and a drop in mean polarization magnitude when entering this phase. However, there is still much work to do. Some possible future directions are: quantifying the rate of cluster coalescing and splitting when phase-separated, introducing nonreciprocity in interaction strength $\epsilon_{\alpha\beta}$ rather than equilibrium distance $\sigma_{\alpha\beta}$, the stability of the phase-separated state as nonreciprocity/interaction are increased, and the system's overall behavior at larger temperatures.

ACKNOWLEDGMENTS

I would like to thank Hyunseok Lee and Sunghan Ro for their help with this project. I would also like to thank Mehran Kardar for a great course.

[1] S. Ramaswamy, Active matter, Journal of Statistical Mechanics: Theory and Experiment **2017**, 054002 (2017), arXiv:1705.06269 [cond-mat].

[2] A. Sokolov, I. S. Aranson, J. O. Kessler, and R. E. Goldstein, Concentration Dependence of the Collective Dynamics of Swimming Bacteria, Physical Review Letters **98**, 158102 (2007), publisher: American Physical Society.

[3] M. C. Marchetti, J. F. Joanny, S. Ramaswamy, T. B. Liverpool, J. Prost, M. Rao, and R. A. Simha, Hydrodynamics of soft active matter, Reviews of Modern Physics **85**, 1143 (2013), publisher: American Physical Society.

[4] D. Banerjee, A. Souslov, A. G. Abanov, and V. Vitelli, enOdd viscosity in chiral active fluids, Nature Communications **8**, 1573 (2017).

[5] B. Liebchen and D. Levis, Chiral active matter, Europhysics Letters **139**, 10.1209/0295-5075/ac8f69 (2022).

[6] M. Fruchart, R. Hanai, P. B. Littlewood, and V. Vitelli, enNon-reciprocal phase transitions, Nature **592**, 363 (2021), publisher: Nature Publishing Group.

[7] M. Han, M. Fruchart, C. Scheibner, S. Vaikuntanathan, J. J. de Pablo, and V. Vitelli, enFluctuating hydrodynamics of chiral active fluids, Nature Physics **17**, 1260 (2021), publisher: Nature Publishing Group.

[8] F. Schmidt, B. Liebchen, H. Löwen, and G. Volpe, Light-controlled assembly of active colloidal molecules, The Journal of Chemical Physics **150**, 094905 (2019).

[9] A. Dinelli, J. O'Byrne, A. Curatolo, Y. Zhao, P. Sollich, and J. Tailleur, enNon-reciprocity across scales in active mixtures, Nature Communications **14**, 7035 (2023).

[10] A. Ivlev, J. Bartnick, M. Heinen, C.-R. Du, V. Nosenko, and H. Löwen, Statistical Mechanics where Newton's Third Law is Broken, Physical Review X **5**, 011035 (2015), publisher: American Physical Society.

[11] T. H. Tan, A. Mietke, J. Li, Y. Chen, H. Higinbotham, P. J. Foster, S. Gokhale, J. Dunkel, and N. Fakhri, enOdd dynamics of living chiral crystals, Nature **607**, 287 (2022).

[12] S. Ro, Y. Kafri, M. Kardar, and J. Tailleur, Disorder-Induced Long-Ranged Correlations in Scalar Active Matter, Physical Review Letters **126**, 048003 (2021), publisher: American Physical Society.

[13] M. Ester, H.-P. Kriegel, J. Sander, and X. Xu, A density-based algorithm for discovering clusters in large spatial databases with noise, in *Proceedings of the Second International Conference on Knowledge Discovery and Data Mining*, KDD'96 (AAAI Press, Portland, Oregon, 1996) pp. 226–231.

[14] M. E. Cates and J. Tailleur, enMotility-Induced Phase Separation, Annual Review of Condensed Matter Physics **6**, 219 (2015), publisher: Annual Reviews.